

# Enhancement of Fault Ride through Capability of Doubly Fed Induction Generator Based Wind Energy Conversion System

Mr. Subir Datta  
Assistant Professor

Department of EE, Mizoram,  
University, Aizawl, Mizoram, India

Mr. Ksh. Robert Singh  
Assistant Professor

Department of EE, Mizoram  
University, Aizawl, Mizoram, India

Mr. Subhasish Deb  
Assistant Professor

Department of EE, Mizoram  
University, Aizawl, Mizoram, India

**Abstract—** Doubly Fed Induction Generator (DFIG) is popularly used in Wind Energy Generation Systems. But, performance of DFIG gets degraded during three phase grid fault due to flow of high rotor current that exceeds the fault-ride through capability of the power electronics converters used. In this paper, a new control switching strategy, using a Series Dynamic Resistor (SDR) protection scheme in series with DC Chopper, is proposed to enhance the fault-ride through capability. The DC Chopper converter and proposed SDR protection scheme is analyzed and simulation results, carried out in MATLAB / Simulink environment, have been presented along with discussions. Simulation results show that the proposed method is effective in providing protection to the DFIG under fault condition.

*Index terms -Doubly Fed Induction Generator (DFIG), Rotor Side Converter (RSC), Grid Side Converter (GSC), Pole Placement Technique, WESC, DC-Chopper, Crowbar and Series dynamic resistor etc.*

## I. INTRODUCTION

Now-a-days, with the penetration level of wind power in power system increasing, the control strategies of wind farm during grid faults and the impacts on the reliable operation of power system have become a hot research topic in the wind power field. In more and more countries, the ability of low voltage ride-through (LVRT) is required in the grid codes for connecting wind farm into power grid [1]. For wind power generation systems, the doubly-fed induction generator (DFIG), with its variable wind speed tracking performance, and relatively low cost compared to fully rated converter wind power generation system, e.g., permanent-magnet synchronous generator (PMSG), is a popular wind generation concept. However, a significant disadvantage of the DFIG is its vulnerability to grid disturbances because the stator windings are connected directly to the grid through a transformer and switchgear with only the rotor-side buffered from the grid via a partially rated converter. Therefore, as to protect the wind farm from interruptions due to onshore grid faults and wind farm faults, crowbar protects the induction generator and associated power electronics. This is widely used in industrial applications. Doubly-fed induction generator (DFIG) is mostly used in the commercial MW-class wind power system, for the rated capacity of the convertor needed in the wind generation system based on DFIG is just about 20-

kinds of generators based wind energy systems, wind turbine with DFIG is difficult to achieve LVRT for its weak ability to withstand grid voltage disturbances [3-4]. In order to keep DFIG connecting to power grid during faults, rotor side crowbar protection as a simple but effective method against surge current caused by sudden dip of grid voltage during LVRT periods is commonly used. A major disadvantage of crowbar protection is that the rotor side converter (RSC) has to be disabled when using the crowbar and the generator consumes reactive power leading to deterioration of grid voltage. In line with developing fault ride-through (FRT) requirements, an active crowbar control scheme is proposed [5], [6] to shorten the time the crowbar is in operation but this does not avoid the reactive power consumption. In such a situation, one would have expected the grid side converter to provide the required reactive power to support the grid. Unfortunately however, the GSC is limited in the amount of reactive power it can generate and may not generate adequate reactive power needed. As a result, static and dynamic VAR compensators or STATCOMs are sometimes installed at the DFIGs terminals to provide reactive power during the grid faults [7-9]. In [10, 11, 12, 13] an additional series connected converter and in [14, 15], a dynamic voltage restorer is employed for improve the FRT capability of the DFIG. However, all these make the control systems complex or increase the issues with control coordination between normal and fault operation. A series topology is proposed [16] to drop rotor circuit voltage hence limiting the rotor current. In the present paper, a new control switching scheme has been proposed to enhance the fault ride through capability of the DFIG by extending the work described in [16]. A proposed switching strategy is implemented by incorporating control of duty cycle of the ON-OFF switch connected in parallel with a fixed resistor; Schematic of the scheme is given in Fig-8. The proposed scheme has been applied to a 1.5MW variable speed wind turbine-DFIG system. The paper has been organized as follows: Modelling & control of the DFIG wind turbine, Vector Control of DFIG Wind turbine and Converter protection schemes are presented in Sections II, III and IV respectively. Simulation results, obtained using MATLAB/Simulink (MATLAB-2013b), have been presented in section V. Finally, conclusions are drawn in section VI.

**II. MODELING AND CONTROL OF THE DFIG WIND TURBINE**

Figure1 shows the basic structure of a DFIG wind turbine. The DFIG is a wound rotor induction machine which is connected to the grid through both stator and rotor terminals. The stator is directly connected to the grid, while the rotor is connected via a PWM back-to-back converter, which consists of rotor side converter (RSC) and a grid side converter (GSC) [17].

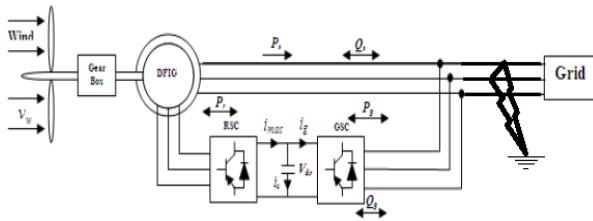


Figure 1 Structure of the DFIG based wind system.

**A. Modeling of the DFIG**

A doubly fed induction generator is a wound-rotor doubly-fed electric machine and has several advantages over a conventional induction machine in wind power applications [18]. The operating principle of a DFIM can be analyzed using the classic theory of rotating fields and the well-known d-q model, as well as both three-to-two and two-to-three phase axes transformations [19]. The dynamic voltages and fluxes equations in the arbitrary d-q reference frame [19]:

$$\left. \begin{aligned} V_{sd} &= R_s i_{sd} + \frac{d}{dt} \phi_{sd} - \omega_s \phi_{sq} \\ V_{sq} &= R_s i_{sq} + \frac{d}{dt} \phi_{sq} + \omega_s \phi_{sd} \\ V_{rd} &= R_r i_{rd} + \frac{d}{dt} \phi_{rd} - (\omega_s - \omega) \phi_{rq} \\ V_{rq} &= R_r i_{rq} + \frac{d}{dt} \phi_{rq} + (\omega_s - \omega) \phi_{rd} \end{aligned} \right\} \quad (1)$$

The flux linkages are given by:

$$\left. \begin{aligned} \phi_{sd} &= L_s i_{sd} + L_m i_{rd} \\ \phi_{sq} &= L_s i_{sq} + L_m i_{rq} \\ \phi_{rd} &= L_r i_{rd} + L_m i_{sd} \\ \phi_{rq} &= L_r i_{rq} + L_m i_{sq} \end{aligned} \right\} \quad (2)$$

The electromagnetic torque of the DFIG can be expressed as follow:

$$T_{em} = \frac{3}{2} * \frac{P}{2} * (\lambda_{ds} * i_{qs} - \lambda_{qs} * i_{ds}) \quad (3)$$

The active and reactive stator power can be expressed as [21]:

$$\left. \begin{aligned} P_s &= \frac{3}{2} (V_{ds} i_{ds} + V_{qs} i_{qs}) \\ Q_s &= \frac{3}{2} (V_{qs} i_{ds} - V_{ds} i_{qs}) \end{aligned} \right\} \quad (4)$$

**III. VECTOR CONTROL OF THE DFIG WIND TURBINE**

The Vector control of a DFIG wind turbine is achieved by controlling the RSC and the GSC. RSC is controlled in the aim to regulate independently the stator active power  $P_s$  and reactive power  $Q_s$ . The objectives of Controlling the GSC are to keep constant the dc-link voltage  $V_{dc}$ , and to regulate the reactive power  $Q_g$  which is exchanged between the GSC and the grid [20].

**A. Vector-Control scheme of the GSC**

A grid voltage oriented vector-control approach is used to enable independent control of the active and reactive power

flow between the grid and the grid-side converter. The PWM voltage source converter is current regulated, with the d-axis current used to regulate the DC-link voltage and the q-axis current used to regulate the reactive power. Fig.2 shows the schematic of the grid-side PWM voltage source converter.

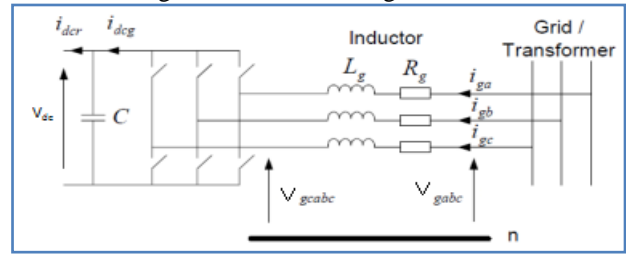


Fig.2 Grid-side PWM voltage source converter

The voltage balance across the inductor

$$\begin{bmatrix} V_{ga} \\ V_{gb} \\ V_{gc} \end{bmatrix} = R_g \begin{bmatrix} i_{ga} \\ i_{gb} \\ i_{gc} \end{bmatrix} + L_g \frac{d}{dt} \begin{bmatrix} i_{ga} \\ i_{gb} \\ i_{gc} \end{bmatrix} + \begin{bmatrix} V_{gca} \\ V_{gcb} \\ V_{gcc} \end{bmatrix} \quad (5)$$

Using the abc-to-dq transformation matrix, the corresponding equation in the dq-reference frame rotating at  $w_e$  is

$$V_{gd} = R_g i_{gd} + L_g \frac{di_{gd}}{dt} - w_e L_g i_{gq} + V_{gcd} \quad (6)$$

$$V_{gq} = R_g i_{gq} + L_g \frac{di_{gq}}{dt} + w_e L_g i_{gd} + V_{gqc} \quad (7)$$

The active  $P_s$  and  $Q_s$  power flow between the grid and grid side converter are [21]

$$P_g = \frac{3}{2} (V_{gd} i_{gd} + V_{gd} i_{gq}) \quad (8)$$

$$Q_g = \frac{3}{2} (V_{gq} i_{gd} - V_{gd} i_{gq}) \quad (9)$$

The angular position  $\theta_e$  of grid voltage is calculated as

$$\theta_e = \int w_e dt = \tan^{-1} \frac{V_{g\beta}}{V_{g\alpha}} \quad (10)$$

where  $V_{g\alpha}$  and  $V_{g\beta}$  are the stationary dq-axis grid voltage components.

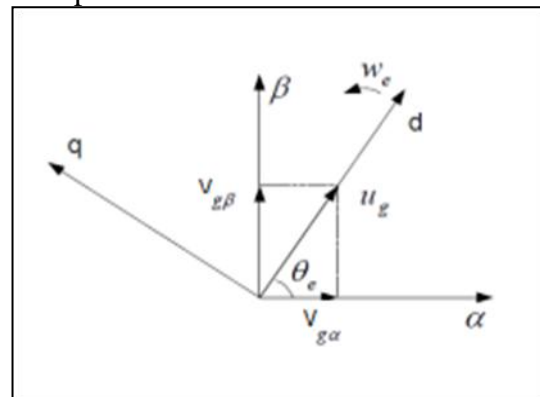


Fig. 3(a) Vector diagram for GSC

Aligning the d-axis of the reference frame along the grid voltage position given by (10), as shown in fig. 3a,  $V_{gq}$  is zero, and the amplitude of the grid voltage  $V_{ds}$  is constant. The active and reactive power flow between the grid and the grid-side converter will be proportional to  $i_{gd}$  and  $i_{gq}$  respectively.

Fig.4 shows the vector control scheme for grid side PWM voltage control converter.

$$P_g = \frac{3}{2} V_{gd} i_{gd} \tag{11}$$

$$Q_g = -\frac{3}{2} V_{gd} i_{gq} \tag{12}$$

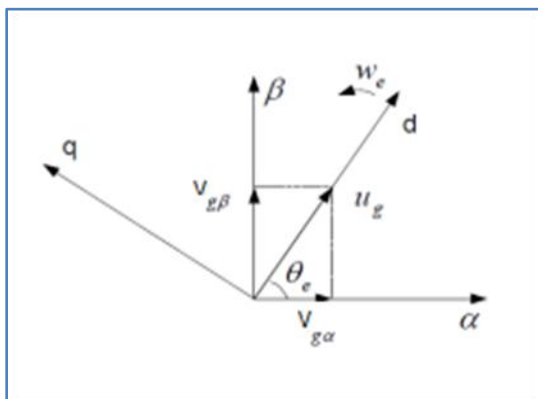


Fig. 3(b) Vector diagram for RSC

**B. Vector-Control scheme of the RSC**

The RSC of Doubly fed induction generator is controlled in a synchronously rotating dq-axis frame, with the d-axis oriented along the stator-flux vector position. The PWM voltage source converter is current regulated with the d-axis current used to regulate the stator reactive power and q-axis current used to regulate the stator active power.

The stator flux angular position  $\theta_s$  is calculated from [21]

$$\left. \begin{aligned} \Psi_{\alpha s} &= \int (V_{\alpha s} - R_s i_{\alpha s}) dt \\ \Psi_{\beta s} &= \int (V_{\beta s} - R_s i_{\beta s}) dt \\ \theta_s &= \int \omega_s dt = \tan^{-1} \left( \frac{\Psi_{\beta s}}{\Psi_{\alpha s}} \right) \end{aligned} \right\} \tag{13}$$

Aligning the d-axis of the reference frame along the stator-flux vector position, as shown in fig. 3b, gives a result that  $\Psi_{qs}$  is zero. With this consideration, the DFIG model may be written as [21]:

$$\left. \begin{aligned} V_{ds} &= 0; & V_s &= V_{qs} = \omega_s \Psi_{ds} \\ V_{dr} &= R_r i_{dr} + \sigma L_r \frac{di_{dr}}{dt} - w_{slip} \sigma L_r i_{qr} \\ V_{qr} &= R_r i_{qr} + \sigma L_r \frac{di_{qr}}{dt} + w_{slip} (L_{mm} i_{ms} + \sigma L_r i_{dr}) \\ \Psi_s &= \Psi_{ds} = i_{ms} = L_s i_{ds} + L_m i_{dr} \\ 0 &= L_s i_{qs} + L_m i_{qr}, & \Psi_{dr} &= \frac{L_m^2}{L_s} i_{ms} + \sigma L_r i_{dr} \\ & & \Psi_{qr} &= \sigma L_r i_{qr} \end{aligned} \right\} \tag{14}$$

where,

$$w_s = w_e; w_{slip} = w_s - w_r; \sigma = 1 - \frac{L_m^2}{L_s L_r} \text{ and } L_{mm} = \frac{L_m^2}{L_s}$$

The stator-side active  $P_s$  and reactive  $Q_s$  power flow are

$$P_s = -\frac{3}{2} \left( \frac{L_m}{L_s} V_s i_{qr} \right) \tag{15}$$

$$Q_s = \frac{3}{2} V_s \left( \frac{V_s}{w_s L_s} - \frac{L_m}{L_s} i_{dr} \right) \tag{16}$$

Due to constant stator voltage, the stator-side active power and reactive power are controlled via  $i_{qr}$  and  $i_{dr}$  respectively. Fig. 5 shows the vector-control scheme for rotor-side PWM voltage source converter.

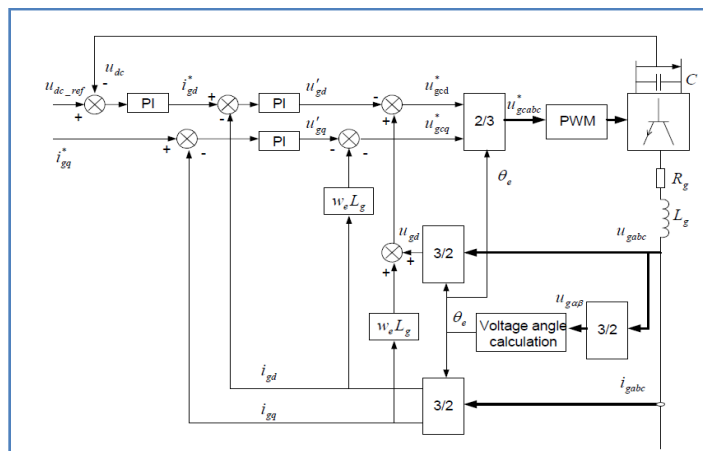


Fig. 4 Vector-control structures for GSC

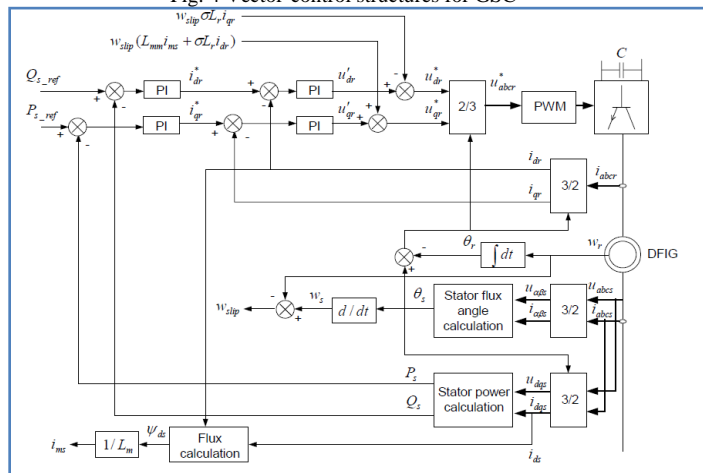


Fig.5 Vector-control structures for RSC

**IV. CONVERTER PROTECTION SCHEMES FOR GRID CONNECTED DFIG BASED WESC**

**A. Crowbar Protection Scheme**

Crowbar protection scheme, as shown in fig.6, has been used to prevent DFIG based wind power generation system under grid fault. A crowbar is a set of resistors that are connected in parallel with the rotor winding on occurrence of an interruption, bypassing the RSC. When the crowbar is triggered, the rotor side converter is disabled and bypassed, and therefore, the independent controllability of active and reactive power is lost. Generator magnetization in this case is supplied from the stator instead of being supplied from the rotor circuit. Since the grid side converter is not directly connected to the rotor windings, when large transient currents appear, this converter is not blocked for protection. Therefore, the DFIG behaves as a conventional squirrel cage induction generator (SCIG) with an increased rotor resistance. By inserting the external resistance, i.e., crowbar resistance into the rotor circuit during grid faults, the pull-out torque of the SCIG is moved into the range of higher speeds [22]. The dynamic stability of the SCIG is thus dramatically improved by increasing the external resistance [23]. When the crowbar protection scheme is removed, the rotor side converter is

enabled again to control independently the active and reactive power.

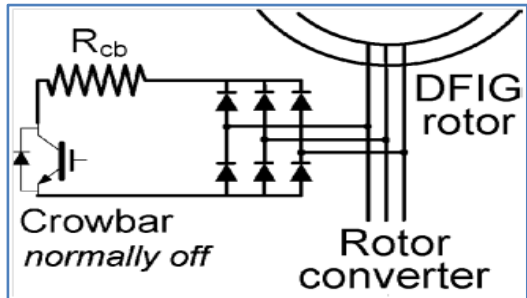


Fig.6 Crowbar Circuit [28]

**B. DC-Chopper Protection Scheme**

A chopper or braking resistor (dumped load) is connected in parallel with the dc-link capacitor to limit the overcharge during low grid voltage. It protects the IGBTs from overvoltage and can dissipate energy, but this has no effect on the rotor current. The DC Chopper protection circuit and switching strategy are shown in fig.8 and fig.7 respectively. The chopper facilitates a voltage-raising action from the converter terminals during the fault ride through (FRT), and thereby enabling a faster regain of the control of the DC link voltage [24, 25 & 26]. A power converter which is operated by pulse width modulation (PWM) technique is almost a standard to drive an electric machine. When a disturbance occurs in the grid, the DC voltage becomes very high that goes beyond the rated value which may cause damage to the semiconductor devices. The protective device in this scheme is a simple chopper circuit. The pulse signal to trigger the IGBT is activated when  $V_{dc}$  exceeds  $V_{dc-max}$ , and thus, the chopper is turned on and the energy is dissipated by the internal resistance. It is also used as protection for the dc-link capacitor in full rated converter topologies, for example, PMSGs [27].

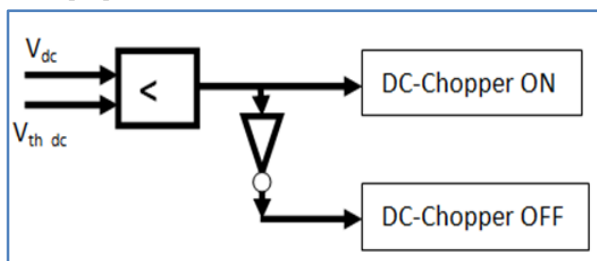


Fig.7. Switching strategy of DC Chopper protection circuit

**C. Series Dynamic Resistor**

Series dynamic resistor (SDR) is connected in series with the rotor winding to limit the rotor overcurrent during low grid voltage. It is controlled by IGBT based power electronic switch as shown in fig.8. During normal operation of the whole system, the power electronic switch is ON and the resistor is bypassed where as during grid fault condition, the switch is OFF and the resistor is connected in series to the rotor winding. The crowbar and DC-link chopper are shunt-connected and control the voltage whereas the SDR is series connected and control the current magnitude directly. Moreover, with the SDR, the high voltage will be shared by

the resistance because of the series topology; therefore, the induced overvoltage may not lead to the loss of converter control. Therefore, it not only controls the rotor overvoltage but also limits high rotor current. In addition, the limited current can reduce the charging current to the dc-link capacitor, hence avoiding dc-link overvoltage. Fig.9 shows the switching strategy to turn OFF/ ON the power electronics device of SDR.

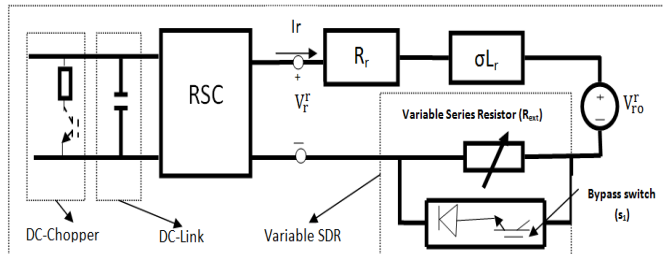


Fig.8 DFIG rotor equivalent circuit with DC-Chopper and VSDR

**D. Proposed switching strategy for SDR**

In the SDR, when  $S_1$  is turn ON,

$$V_r^r = I_r * R_r + \frac{d}{dt} (I_r) * \sigma * L_r + V_{ro}^r \tag{17}$$

When  $S_1$  is turn OFF,

$$V_{ro}^r = I_r * R_r + \frac{d}{dt} (I_r) * \sigma * L_r + V_{ro}^r + I_r * R_{ext} \tag{18}$$

With combination of equations (17) & (18),

$$V_{ro}^r = I_r * R_r + \frac{d}{dt} (I_r) * \sigma * L_r + V_{ro}^r + (1 - d) I_r * R_{ext} \tag{19}$$

where,  $d = \text{duty cycle} = \frac{I_r^{ref}}{I_r}$  and  $I_r^{ref}$  = rotor reference current which is generated from equation (15) and  $I_r$  = magnitude of actual current. The detail control scheme is shown in fig.9.

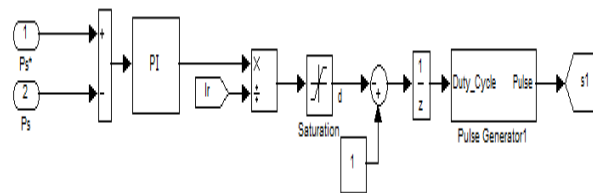


Fig.9. Control scheme of SDR

**IV. SIMULATION RESULTS AND DISCUSSION**

The model of the complete system has been prepared using MATLAB/Simulink (Matlab-2013b) Power System Blocksets (PSB) by combining the respective blocks for each of the individual components systems and simulations has been carried out for the said model. All relevant parameters are given in the Appendix. Rated wind velocity (i.e. 12 m/s) is considered to carry out this study. This study consists in controlling both of RSC and GSC of a WECS based on the DFIG under three phase grid fault condition. The time responses of: (i) Reference & actual speed (wr),  $C_p$  (power Co-efficient) (ii) Reference & actual stator power ( $P_s$ ), Reference & actual reactive power ( $Q_s$ ) and mechanical & electrical torque ( $T_m$  &  $T_e$ ), (iii) d-axis rotor current ( $I_{dr}$ ) and q-axis rotor current ( $I_{qr}$ ), (iv) d-axis stator voltage ( $V_{ds}$ ), q-axis stator voltage ( $V_{qs}$ ) and d-axis stator flux ( $\psi_{ds}$ ) (v) Reference & actual DC-link voltage ( $V_{dc}$ ), (vi) Rotor Power ( $P_r$ ), in response

to the three phase grid fault, are shown respectively in Figures 10(a,b), 11(a,b,c), 12(a,b), 13(a,b,c),14,15 and figures 16(a,b), 17 (a,b,c), 18(a,b), 19(a, b,c), 20, 21 without and with protection schemes respectively.

**A. Effect of Three Phase Grid Short Circuit fault without Protection Scheme**

To demonstrate the effects of three phase grid short circuit fault, a DFIG based wind turbine together with a grid has been simulated in Matlab/simulink platform using a detailed circuitry time domain model. This example is aimed to show the effects of a short circuit fault without any countermeasures on the converter and generator side. As can be seen in figs.10-15 the grid three phase fault can lead to considerable over speed, under voltage, over currents and over-dc link voltage putting the whole system under stress.

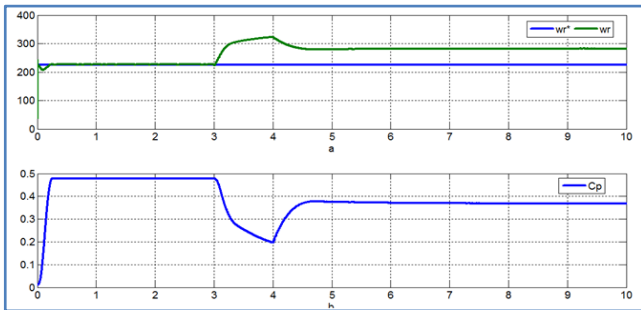


Fig.10- Speed & Cp without protection Scheme

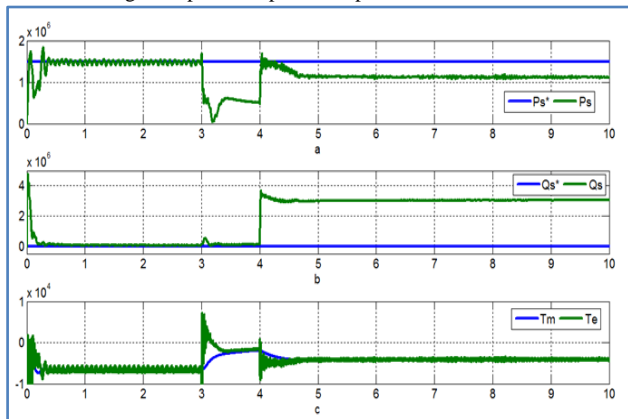


Fig.11 active & reactive power & Torque without protection Scheme

Fig.12 Rotor Current without protection Scheme

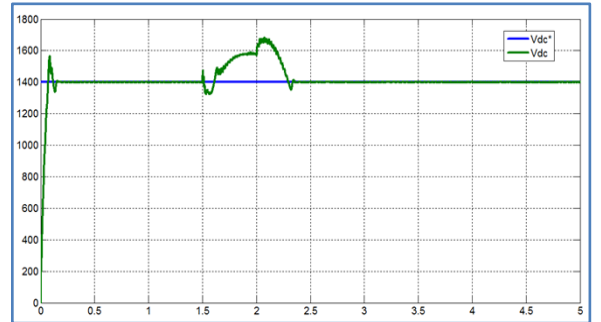
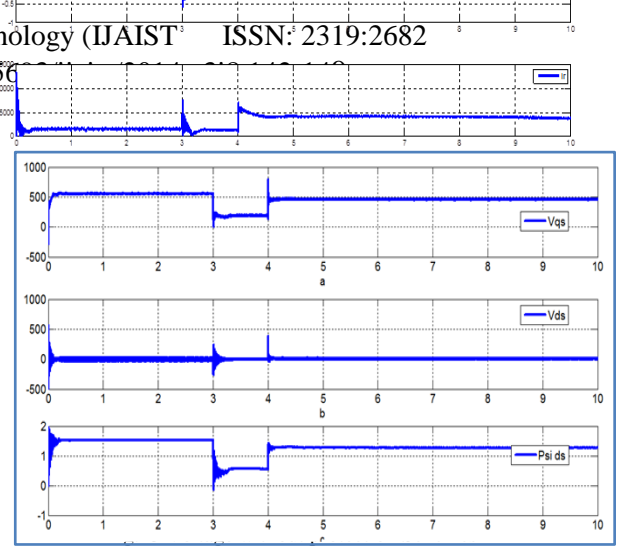


Fig.14 Dc-Voltage without protection Schemes

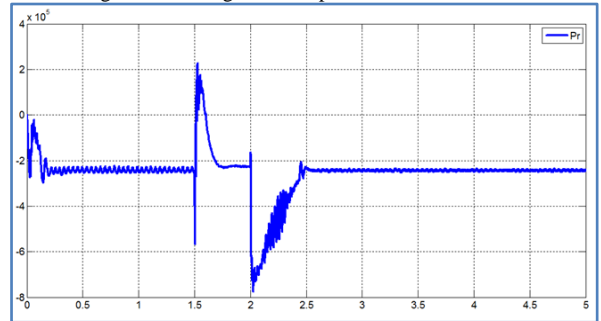
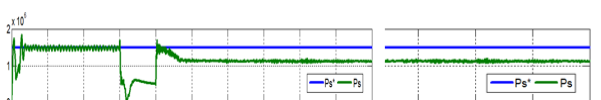


Fig.15 Pr without protection Schemes

Three Phase Fault is applied for 1s to the infinite bus at t=3s. The same grid fault can cause voltage sag at the connection of the WECS as shown in fig.13. Such a voltage sag results in mismatch between mechanical power and the electrical power, which initiates the machine current transients, the over dc-link voltage and a change in speed as shown in figures 12,14, 10 respectively. Fig. 12 shows that the rotor current exceeds its rated limiting value even after the grids fault is cleared. Therefore, the RSC must be blocked to avoid being destroyed from over current in the rotor circuit. As a result, DFIG lost its controllability and WECS must be disconnected from the grid to protect the system from over stress. Therefore, protection scheme is necessary to protect the converter of a DFIG based grid connected wind energy conversion system during and after three phase grid fault condition.

**B. Effect of Three Phase Grid Short Circuit fault with Protection Scheme**

Fig.8 shows a DFIG rotor equivalent circuit for improved fault ride through capability [16]. It contains two protection circuits, DC-chopper and SDR, to avoid DC link





over-voltages and limiting the rotor current during and after grid faults. Immediately after the three phase short circuit fault the DC-link voltage rises to about the threshold value of 1400 V and rotor current also rises above the rated rotor current as shown in figs 10-15, despite the intervention by the protection circuits. To avoid overload, the SDR and DC-chopper is active during and after the grid fault. Figs. 16-21 show the behavior of the DFIG system with both SDR and DC-link chopper protection circuit. As can be seen from the results the RSC has been successfully protected against the overload during the grid fault.

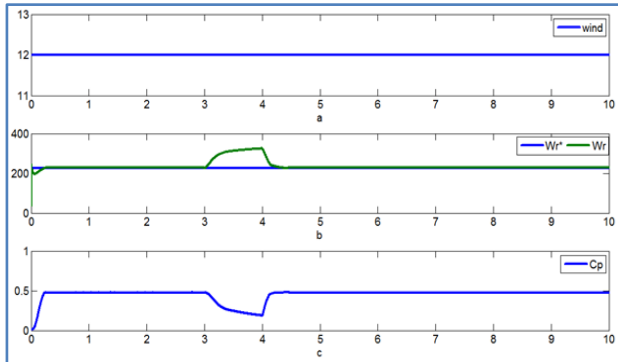


Fig-16 Speed & Cp with protection Scheme

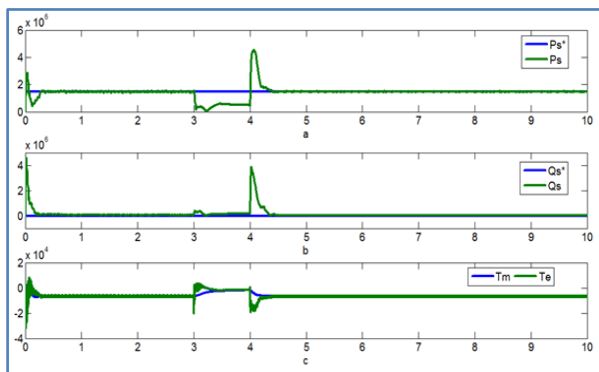


Fig.17 active & reactive power & Torque with protection Scheme

**V. Conclusion**

It is necessary to protect the converter of a DFIG based grid connected wind energy conversion system during and after

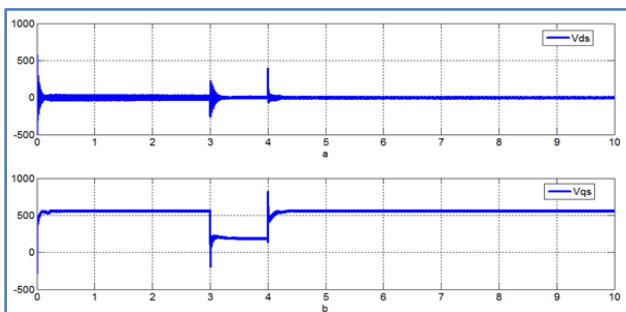


Fig.18 Voltage with protection Schemes

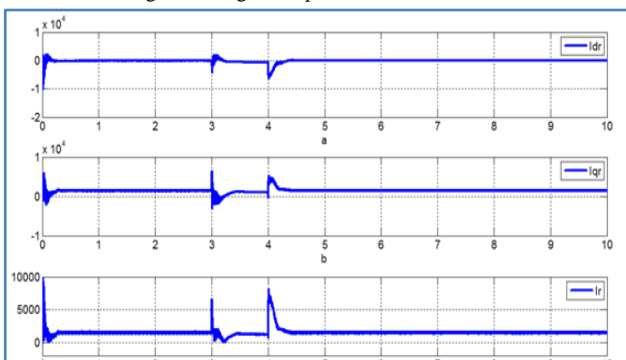


Fig.19 Rotor Current with protection

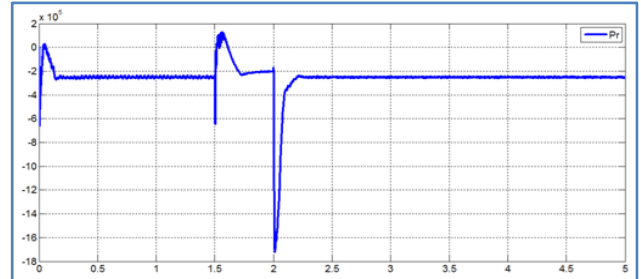


Fig.20 Pr with protection Schemes

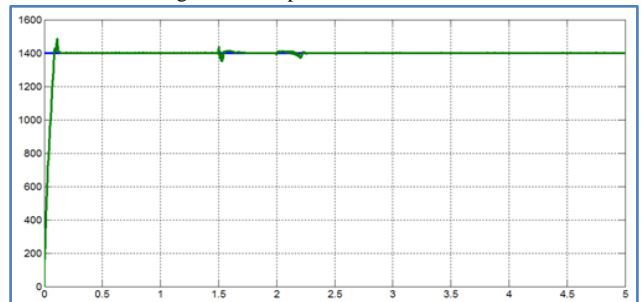


Fig. 21 DC-link voltage with protection Schemes

three phase grid fault condition. In this paper, a new switching strategy based series dynamic resistor protection scheme is used to protect the converter of the DFIG system during and after the fault. The objective of an SDR is to avoid the crowbar protection scheme, to maximize the operation time of the RSC, and to reduce torque fluctuations during protection operation. The rotor current during three phase grid fault condition is presented and rotor voltage expressions, with and without SDR, are given to instruct the switching controller design of the SDR protection scheme. The dc-chopper is used for dc-link overvoltage limitation. During this process, simulation results show that the proposed method enhances DFIG Fault Ride Through capability.

**REFERENCES**

- [1]. M. Tsili, S. Papathanassiou, "A review of grid code technical requirements for wind farms," *IET Renewable Power Generation*, vol.3, iss.3, pp.308-332, Mar. 2009.
- [2]. R. Datta, V. T. Ranganatha, "Variable-speed wind power generation using doubly fed wound rotor induction machine-a comparison with alternative schemes," *IEEE Trans. Energy Conversion*, vol.17, no.3, pp. 414-421, Sep. 2002.
- [3]. D. W. Xiang, L. Ran, P. J. Tavner, S. C. Yang, "Control of a doubly fed induction generator in a wind turbine during grid fault ride-through," *IEEE Trans. Energy Conversion*, vol. 21, no.3, pp. 652-662, Sep. 2006.

[4]. J. Lopez, P. Sanchis, X. Roboam, and L. Marroyo, "Dynamic Behavior of the Doubly Fed Induction Generator During Three-Phase Voltage Dips," *IEEE Trans. Energy conversion*, vol. 22, no. 3, pp. 709-717, Sep. 2007.

[5]. J. Morren and S. W. H. de Haan, "Ridethrough of wind turbines with doubly-fed induction generator during a voltage dip," *IEEE Trans. Energy Convers.*, vol. 20, no. 2, pp. 435-441, Jun. 2005.

[6]. I. Erlich, J. Kretschmann, J. Fortmann, S. Mueller-Engelhardt, and H. Wrede, "Modeling of wind turbines based on doubly-fed induction generators for power system stability studies," *IEEE Trans. Power Syst.*, vol. 22, no. 3, pp. 909-919, Aug. 2007.

[7]. Qiao W, Harley RG, Vanayagamoorthy GK. Coordinated reactive power control of a large wind farm and a STATCOM using heuristic dynamic programming. *IEEE Trans Energy Convers* 2009;24:493-503.

[8]. Amaris H, Alfonso M. Coordinated reactive power management in power networks with wind turbines and FACTS devices. *Energy Convers Manage* 2011;52:2575-86.

[9]. Rahim AHMA, Nowicki EP. Super capacitor energy storage system for fault ride-through of a DFIG wind generation system. *Energy Convers Manage* 2012;59:96-102.

[10]. Abdel-Baqi O, Nasiri A. Series voltage compensation for DFIG wind turbine low voltage ride through solution. *IEEE Trans Energy Convers* 2011;26:272-80.

[11]. Zhang S, Tseng KJ, Choi SS, Nguyen TD and Yao DL, "Advanced control of series voltage compensation to enhance wind turbine ride through", *IEEE Trans Power Electron* 2012;27:763-72.

[12]. Wessels C, Gebhardt F and Fuchs FW, "Fault ride through of a DFIG wind turbine using a dynamic voltage restorer during symmetrical and asymmetrical grid faults", *IEEE Trans Power Electron* 2011;26:807-15.

[13]. Ibrahim AO, Nguyen TH, Lee DC and Kim SC, "A fault ride through technique of DFIG wind turbine systems using dynamic voltage restorers", *IEEE Trans Energy Convers*. 2011; 26: 871-82.

[14]. D. Xiang, R. Li, P. J. Tavner, and S. Yang, "Control of a doubly fed induction generator in a wind turbine during grid fault ride-through," *IEEE Trans. Energy Convers.*, vol. 21, no. 3, pp. 652-662, Sep. 2006.

[15]. P. S. Flannery and G. Venkataramanan, "A fault tolerant doubly fed induction generator wind turbine using a parallel grid side rectifier and series grid side converter," *IEEE Trans. Power Electron.*, vol. 23, no. 3, pp. 1126-1135, May 2008.

[16]. Jin Yang, John E. Fletcher and John O'Reilly, "A Series-Dynamic-Resistor-Based Converter Protection Scheme for Doubly-Fed Induction Generator during Various Fault Conditions," *IEEE Trans. on Energy Conversion*, VOL. 25, NO. 2, pp. 422-432, June 2010.

[17]. L. Qu and W. Qiao, "Constant Power Control of DFIG Wind Turbines With Super capacitor Energy Storage" *IEEE Trans. Ind. Appl.*, vol. 47, no.1, pp. 359-367, Jan/Feb. 2011.

[18]. Milton Kumar Das, S. Chowdhury, S.P. Chowdhury and C.T. Gaunt, "Control of a Grid Connected Doubly-Fed Induction Generators for Wind Energy Conversion", *IEEE, 2009*.

[19]. Krause, O. Wasynczuk, and S. D. Sudhoff, "Analysis of Electric Machinery and Drive Systems," *IEEE Press, Wiley-Interscience, John Wiley & Sons, Inc.*, New Jersey, 2002.

[20]. R. Pena, J.C. Clear, G.M. Asher, "Doubly fed induction generator using back-to-back PWM Converters and its application to variable- speed wind energy generation," *IEE Proc.-Electr. Power Appl.* Vol.143, No.3, May 1996.

[21]. T. Sun, "Power Quality of Grid-Connected Wind Turbines with DFIG and Their Interaction with the Grid," Ph.D thesis, Institute of Energy Technology, Aalborg University, Denmark, May, 2004.

[22]. A. D. Hasan, and G. Michalke, "Fault Ride-Through Capability of DFIG Wind Turbines," *Renewable Energy*, vol.32, pp.1594-1610, 2007.

[23]. V. Akhmatov, "Analysis of Dynamic Behavior of Electric Power Systems with Large Amount of Wind Power," *PhD Thesis*, 2003, Orsted DTU.

[24]. I. Erlich, J. Kretschmann, J. Fortmann, S. Mueller-Engelhardt, and H. Wrede, "Modeling of wind turbines based on doubly-fed induction generators for power system stability studies," *IEEE Trans. Power Syst.*, vol. 22, no. 3, pp. 909-919, Aug. 2007.

[25]. I. Erlich, H. Wrede, and C. Feltes, "Dynamic behavior of DFIG-based wind turbines during grid faults," presented at the Power Convers. Conf., Nagoya, Japan, Apr. 2-5, 2007.

[26]. M. B. C. Salles, K. Hameyer, J. R. Cardoso, A. P. Grilo, and C. Rahmann, "Crowbar system in doubly fed induction wind generators," *Energies Article Journal*, ISSN 1996-1073, vol. 3, pp. 738-753, 2010.

[27]. J. F. Conroy and R. Watson, "Low-voltage ride-through of a full converter wind turbine with permanent magnet generator," *IET Renew. Power Gener.*, vol. 1, no. 3, pp. 182-189, 2007.

[28]. Graham Pannell, David J. Atkinson, and Bashar Zahawi, "Minimum-Threshold Crowbar for a Fault-Ride-Through Grid-Code-Compliant DFIG Wind Turbine," *IEEE Trans On Energy Conversion*, 2010

**Appendices**

**A. Specifications of Doubly fed induction generator**

Rated Capacity = 1.5MW; Optimal (Rated) Rotor speed=2158 rpm(Electrical);Wm (rated)= 225.9 rad/sec (Mech.); No. of poles=4; Frequency=60 Hz ;Ns (synchronous speed)=1800 rpm; Synchronous angular speed (Ws)= 188.5 rad/sec (Mech.); Rated Voltage (Line to line) = 690V;Shaft Inertia=18.7kg.m<sup>2</sup>; Mutual inductance=2.88mH; Rotor referred inductance=2.97mH; Stator inductance=2.93 mH; Rotor referred resistance=2 m-ohm; Stator Resistance=2.3 m-ohm

**B. Specifications of Wind turbine:**

Blade Radius=30.66m; Cut-in/cut-out wind speed=12 m/s; Gear Box=71.28; Rated wind speed=12 m/s; Air density=1.225 kg/m<sup>3</sup>

**C. Specification of converter**

DC-link Voltage=1400V; DC-link capacitor=60mF; Switching frequency=5000 Hz; Sampling time=2e-5

### Authors Profile



**Subir Datta** received the **B.Tech.** and **M.Tech.** degrees from the North Eastern Regional Institute of science & Technology, India in 2008 and National Institute of Technology Silchar, India in 2010 respectively. He is currently an Assistant Professor of Electrical

Department at Mizoram University, India. His research interests include Electric Machine & Drives, Renewable energy and Power Electronics.



**Ksh. Robert Singh** received the **B.Tech.** and **M.E.** Degrees from the A.C College of Engg. & Technology, Tamil Nadu, India in 2003 and Karunya University, Coimbatore India in 2007 respectively. He is currently an Assistant Professor of Electrical

Department at Mizoram University, India. His research interests include Image Processing, Electric Machine & Drives, and Power Electronics.



**Subhasish Deb** received the **B.Tech.** and **M.Tech.** Degrees from the NIT Agartala, India in 2009 and NIT Silchar, India in 2012 respectively. He is currently an Assistant Professor of Electrical Department at Mizoram University, India. His research interests include Power System Deregulation,

Soft computing, Renewable energy and Power Electronics.